Laboratory Investigation (2012) 92, 753–768

Activation of transient receptor potential vanilloid subtype 1 increases expression and permeability of tight junction in normal and hyposecretory submandibular gland

Xin Cong[1,*], Yan Zhang[1,*], Liang Shi[2,3], Ning-Yan Yang[2], Chong Ding[1], Jing Li[2], Qian-Wen Ding[2,4], Yun-Chao Su[1], Ruo-Lan Xiang[1], Li-Ling Wu[1], and Guang-Yan Yu[2]

Tight junction (TJ) is an important structure that regulates material transport through the paracellular pathway across the epithelium, but its significance in salivary physiology and pathogenesis of salivary dysfunctional diseases is not fully understood. We previously demonstrated that a functional transient receptor potential vanilloid subtype 1 (TRPV1) expresses in submandibular gland (SMG). However, association of TRPV1-induced saliva secretion with TJ remains unknown. Here we explored the effect of TRPV1 activation on expression and function of TJ of rabbit SMG *in vitro* and *in vivo*. RT-PCR and western blot analysis revealed that capsaicin upregulated expression of zonula occludin-1 (ZO-1), claudin (Cldn)-3, and -11, but not Cldn-1, -2, -4, -5, and -7 in cultured SMG cells. Capsaicin also increased the entering of 4 kDa FITC-dextran into the acinar lumen, induced redistribution of cytoskeleton F-actin under confocal microscope, and these effects were abolished by preincubation of capsazepine, a TRPV1 antagonist, indicating that activation of TRPV1 increases expression and permeability of TJ in SMG. Additionally, in a hyposecretory model induced by rabbit SMG transplantation, the expression of ZO-1, Cldn-3, and -11 was decreased, whereas other TJs remained unaltered. The structure of TJ was impaired and the width of apical TJs was reduced under transmission electron microscope, concomitant with diminished immunofluorescence of F-actin in peri-apicolateral region, indicating impaired TJ expression and decreased paracellular permeability in the transplanted SMG. Moreover, topical capsaicin cream increased secretion, decreased TJ structural injury, reversed TJ expression levels, and protected F-actin morphology from disarrangement in transplanted SMGs. These data provide the first evidence to demonstrate that TJ components, particularly ZO-1, Cldn-3, and -11 have important roles in secretion of SMG under both physiological and pathophysiological conditions. The injury in TJ integrity was involved in the hypofunctional SMGs, and TRPV1 might be a potential target to improve saliva secretion through modulating expression and function of TJs.

Laboratory Investigation (2012) **92,** 753–768; doi:10.1038/labinvest.2012.12; published online 5 March 2012

KEYWORDS: extracellular signal-regulated kinase 1/2; myosin light chain-2; saliva secretion; submandibular gland; tight junction; transient receptor potential vanilloid subtype 1

Tight junctions (TJs) are cell–cell interactions ubiquitously expressed in epithelium and endothelium, having an essential role in regulating water and solute transport through the paracellular pathway.[1] As a multifunctional protein complex, TJs are composed of transmembrane proteins, like claudin (Cldn) family members, and intracellular scaffold proteins, such as zonula occludin-1 (ZO-1), which link the transmembrane TJ proteins with intracellular actin

[1]Center for Salivary Gland Diseases of Peking University School and Hospital of Stomatology, Department of Physiology and Pathophysiology, Peking University Health Science Center and Key Laboratory of Molecular Cardiovascular Sciences, Ministry of Education, Beijing, China; [2]Department of Oral and Maxillofacial Surgery, Peking University School and Hospital of Stomatology, Beijing, China; [3]Department of Oral and Maxillofacial Surgery, Qilu Hospital, Shandong University, Shandong, China and [4]Department of Dental Emergency, Beijing Stomatological Hospital, Capital Medical University, Beijing, China

Correspondence: Professor LL Wu, MD, Center for Salivary Gland Diseases of Peking University School and Hospital of Stomatology, Department of Physiology and Pathophysiology, Peking University Health Science Center and Key Laboratory of Molecular Cardiovascular Sciences, Ministry of Education, 38 Xueyuan Road, Haidian District, Beijing 100191, China or Professor GY Yu, DDS, PhD, Department of Oral and Maxillofacial Surgery, Peking University School and Hospital of Stomatology, 22 South Zhongguancun Avenue, Haidian District, Beijing 100081, China.

E-mail: pathophy@bjmu.edu.cn or gyyu@263.net

*These authors contributed equally to this work.

Received 23 August 2011; revised 26 December 2011; accepted 3 January 2012

cytoskeleton.[1,2] It has been shown that TJs not only serve as the main structure that contributes to cell polarity, but also form the primary barrier against the diffusion of solutes via paracellular pathway. TJs dynamically alter their morphology, as well as paracellular permeability in response to diverse physiological and pathological factors. To date, several studies have shown the significant impacts of TJs on airway, intestinal, renal epithelium, and brain blood artery endothelium, indicating a strong correlation between the TJs and polarized secretions, barriers against interstitial fluids, absorption, and the blood–brain barrier functions, respectively.[3–6] Although the previous studies have demonstrated that some of TJ proteins are expressed in human, rat, and mouse submandibular glands (SMGs),[7–11] their functions and the related regulatory mechanism on saliva secretion remain to be elucidated.

The secretion of SMG is primarily controlled by neurotransmitters released from sympathetic and parasympathetic nerves. In addition, some peptides, such as substance P and neuropeptide Y, are also involved in regulating saliva secretion through their receptors.[12] Transient receptor potential vanilloid subtype 1 (TRPV1) is a ligand-gated, nonselective cation channel, which can be activated by heat ($>43\,^{\circ}C$) and low pH, as well as capsaicin, the main pungent ingredient in hot chilli peppers.[13] Our previous study demonstrated that TRPV1 is expressed in both human and rabbit SMGs, and TRPV1 activation by capsaicin increases saliva secretion.[14,15] These results indicate that activation of TRPV1 may be part of a novel pathway for regulating SMG secretion. However, the exact secretory mechanism mediated by TRPV1 is not fully understood. A previous study has demonstrated that capsaicin increases the TJ paracellular permeability in human intestinal Caco-2 cells;[16] we therefore speculated that activation of TRPV1 might induce saliva secretion by modulating the expression and function of TJs.

Dry eye syndrome is a common ophthalmological disorder characterized by reduced amount of or lack of tears and has serious complications, including corneal damage and even loss of sight. The autotransplantation of SMG with implantation of Wharton's duct into the upper conjunctival fornix is an effective approach for treating severe dry eye syndrome, which provides a continuous, endogenous source of ocular lubrication.[17] However, the transplanted SMGs experience hyposecretion from 5 days to 3 months after surgery, which may lead to obstruction of Wharton's duct or even to transplantation failure in some patients.[18] It is vital to investigate the pathogenesis of the submandibular hypofunction. By establishing a rabbit SMG autotransplantation model, our previous study showed that topical capsaicin cream increased secretion of hypofunctional glands partly through upregulating the levels of TRPV1 and aquaporin 5;[19] however, the alteration of the TJs in hypofunctional transplanted SMGs, as well as the effect of capsaicin on TJs, is still unknown.

Therefore, the present study was designed to explore the followings: (1) the effect of TRPV1 activation on the expression and function of TJs in normal rabbit SMG; (2) the change of TJs in the transplanted SMGs; and (3) whether capsaicin increased secretion of the hypofunctional SMGs through improving expression and modulating structure of TJs. These may allow us to further understand the physiological and pathophysiological significance of TRPV1-regulated TJs in SMG *in vivo* and *in vitro*.

MATERIALS AND METHODS

Reagents and Antibodies

Capsaicin, capsazepine (CPZ), 4 and 40 kDa FITC-dextran, PD98059, ML-7, and FITC-labeled phalloidin were purchased from Sigma-Aldrich (Sigma-Aldrich, MO, USA). Antibodies to extracellular signal-regulated kinase 1/2 (ERK1/2), phospho-ERK1/2 (p-ERK1/2), myosin light chain 2 (MLC2), phospho-MLC2 (p-MLC2), actin, and FITC-conjugated secondary antibodies were from Santa Cruz Biotechnology (Santa Cruz, CA, USA). Antibodies to ZO-1, Cldn-3, -11, and TRITC-labeled Cldn-4 were from Zymed (Zymed/Invitrogen, Carlsbad, CA, USA). Zostrix cream with 0.075% capsaicin was obtained from Medicis Pharmaceutical (Phoenix, PA, USA).

Cell Culture

Primary cells of rabbit SMG were cultured by enzymatic digestion as described previously.[15] Briefly, neonatal rabbits (1-day-old) were anesthetized with sodium pentobarbital (50 mg/kg, intraperitoneal). The SMG was excised and dissected free of connective tissue, rinsed twice with ice-cold phosphate buffer saline, minced, and then digested in medium containing 0.1% pancreatin and 0.025% collagenase for 20 min at 37 °C. The cell suspension was centrifuged at 1000 *g* for 5 min and washed twice with Dulbecco's modified Eagle's medium (DMEM) containing 5% fetal bovine serum (FBS) to terminate the digestion. Then, the cells were resuspended in DMEM with 15% FBS, filtered through a 150-mesh bolting cloth, and cultured in 15% FBS–DMEM in a humidified incubator with 5% CO_2 at 37 °C for 24 h. The cells were stained with cytokeratins 17 and 20 (DakoCytomation, Glostrup, Denmark) and epithelial origin was confirmed. The cells were serum starved for 12 h before experiments and then treated with and without 10 μM capsaicin for the indicated times.

Paracellular Permeability Assay

Healthy male New Zealand rabbits (weighing 2.4 ± 0.3 kg) were used. The paracellular permeability assay was performed as described previously, with a minor modification.[20] Briefly, rabbits were killed under sodium pentobarbital (20 mg/kg, in ear vein) anesthesia. The SMGs were immediately removed, cut into small pieces, and then placed in a chamber (Costar, Corning, NY, USA) with Krebs-Ringer Hepes (KRH) solution (containing 120 mM NaCl, 5.4 mM KCl, 1 mM $CaCl_2$,

0.8 mM $MgCl_2$, 11.1 mM glucose, 20 mM HEPES, pH 7.4), aerated with 95% O_2 at 37 °C. FITC-dextran, 4 or 40 kDa, was respectively added to KRH solution to a final concentration of 1 mg/ml, and the tissues were observed under a confocal microscope (Leica TCS SP2, Wetzlar, Germany). Capsaicin (10 μM) was added into the incubation solution and the pictures of acini were caught by the microscope every 5 s. For quantitative measurement of the paracellular permeability, 10 fields from each picture were randomly picked and the fluorescence intensity surrounding each acinar islet was measured by the ImageJ Software (National Institutes of Health). Data were represented as statistical analysis at 300 s normalized to 0 s (Con).

SMG Transplantation

The SMG autotransplantation was performed as described previously.[21] Briefly, under sodium pentobarbital (20 mg/kg, in ear vein) anesthesia, the right SMG with its Wharton's duct and related blood vessels were isolated from the submaxillary triangle to the left temporal region. The artery of the gland was revascularized to the distal part of the external carotid artery, and the vein to the temporal vein. A polyethylene tube was inserted into Wharton's duct and left outside the temporal skin for secretion measurement. Rabbits were randomly divided into three groups: control (without transplantation), transplantation, and capsaicin (transplantation with topical capsaicin cream treatment). Zostrix cream (0.2 g) with 0.075% capsaicin or vehicle cream was spread over the skin (2×2 cm^2) covering the gland twice a day from post-operative days 1–7. On day 7, glands were removed under anesthesia for further investigation.

Preparation of RNA and RT-PCR

Total RNA was extracted with Trizol (Invitrogen) according to manufacturer's instructions. cDNA was prepared from 4 μg of total RNA with M-MLV reverse-transcriptase (Promega, Madison, WI, USA). The primers for TJs (Table 1) were designed according to mRNA sequence of human ZO-1, Cldn-1, -2, -3, -4, -5, -6, -7, and -11. Human SMG tissues were used as a positive control, which were obtained from the patients who had primary oral squamous cell carcinoma and were undergoing functional neck dissection as part of the surgical treatment. The band densities of the amplification products on 1.5% agarose gel were quantitated by a gel electrophoresis image system (Leica 550IW, Leica). All experimental procedures were approved by the Ethics Committee of Peking University Health Science Center and were in accordance with the Guidance of the Ministry of Public Health for the Care and Use of Laboratory Animals. All participants signed an informed consent document before tissue collection.

Western Blot

The cultured cells or SMG tissues were homogenized with lysis buffer (containing 50 mM Tris-HCl, 150 mM NaCl, 1 mM EDTA, 1 mM phenylmethylsulfonyl fluoride, 1% Triton X-100, 0.1% SDS, and 0.1% sodium deoxycholate, pH 7.2) by use of a polytron homogenizer as described previously.[19] The homogenate was centrifuged at 1000 *g* for 10 min at 4 °C, and the supernatant was collected. The concentration of proteins was measured by the Bradford method. Crude protein extract (40 μg) was separated on a 9% SDS-PAGE and transferred to polyvinylidene difluoride membrane. The membranes were blocked with 5% non-fat milk, probed with primary antibodies at 4 °C overnight, and then incubated with horseradish peroxidase-conjugated secondary antibodies. Immunoreactive bands were visualized with enhanced chemiluminescence (Pierce, Rockford, IL, USA) and exposed to an X-OMATTAM film (Kodak, Rochester, NY, USA). The density of bands was scanned and quantified with the Leica 550IW image analysis system.

Immunofluorescence

The SMG cells or frozen sections (6 μm) of SMGs were fixed in 4% paraformaldehyde, incubated in 1% bovine serum albumin for 30 min, and then, the cells or slides were stained

Table 1 Primers for rabbit TJ components mRNA

Gene	Upper primer (5′–3′)	Lower primer (5′–3′)	Size (bp)	Tm (°C)
ZO-1	CCTTCAGCTGTGGAAGAGGATG	AGCTCCACAGGCTTCAGGAAC	287	59.8
Cldn-1	GCAGAAGATGAGGATGGCTGT	CCTTGGTGTTGGGTAAGAGGT	253	59.8
Cldn-2	GCCATGATGGTGACATCCAGT	TCAGGCACCAGTGGTGAGTAG	218	59.8
Cldn-3	GGACTTCTACAACCCCGTGGT	AGACGTAGTCCTTGCGGTCGT	230	59.8
Cldn-4	CAAGGCCAAGACCATGATCGT	GCGGAGTAAGGCTTGTCTGTG	246	59.8
Cldn-5	GGCACATGCAGTGCAAAGTGT	ATGTTGGCGAACCAGCAGAGT	247	59.8
Cldn-6	GGTGCTCACCTCTGGGATTGT	GCAGGGGCAGATGTTGAGTAG	267	59.8
Cldn-7	CTCGAGCCCTAATGGTGGTCT	CCCAGGACAGGAACAGGAGAG	326	59.8
Cldn-11	CTGATGATTGCTGCCTCGGT	ACCAATCCAGCCTGCATACAG	243	59.8

Abbreviations: Cldn, claudin; TJ, tight junction; ZO-1, zonula occludin-1.

with FITC-labeled phalloidin or TRITC-labeled Cldn-4 for 2 h at 37 °C. The slides were also stained with antibodies for ZO-1 or Cldn-3 at 4 °C overnight, and then incubated with FITC-labeled secondary antibody for 2 h at 37 °C. Nuclei were stained with DAPI (Sigma-Aldrich). Fluorescence images were taken with a confocal microscope (Leica TCS SP2). The quantitative measurement of F-actin was done by using the Leica TCS SP2 software (LAS AF). For SMG cells, the fluorescent intensities of F-actin in 10 random cells from each group were averaged, and data were reported as the fluorescent intensity of F-actin in the peri-membrane area and the ratio of peri-membrane to total F-actin. For SMG tissue sections, the fluorescent intensities of F-actin from five sections of 10 randomly selected acini in each section in control, transplanted, and capsaicin groups were averaged. Data were reported as the fluorescent intensity of F-actin in the peri-apicolateral region, and the ratio of F-actin in the peri-apicolateral region of acinar cells to total F-actin.

Saliva Secretion Measurement

Saliva secretion from the transplanted and control rabbits was measured between 09:00 and 10:00 h at resting and conscious conditions. Five minutes after the capsaicin or vehicle cream application, the length of filter paper (35 mm × 5 mm) moistened by saliva from the tube inserted into Wharton's duct was measured for 5 min as described by Schirmer's test.[22]

Transmission Electron Microscopy

The SMG specimens were fixed in 2% paraformaldehyde–1.25% glutaraldehyde. Ultrathin sections were stained with uranyl acetate and lead citrate, and examined with a transmission electron microscope (H-7000 electron microscope, HITACHI, Tokyo, Japan). Each image was taken under the same conditions, such as brightness and contrast, for a better comparison on TJ density among different groups. For morphometric analysis,[23] the distance between neighboring TJs (shown as the width of apical TJs) from 5 sections of 10 randomly selected fields in each section in control, transplanted, and capsaicin glands were measured and averaged by the use of ImageJ software (NIH) blindly by two examiners.

Statistical Analysis

Data are presented as mean ± s.d. Differences among multiple groups were analyzed by one-way ANOVA and followed by Bonferroni's tests using GraphPad Prism 5.0 software. Values of $P<0.05$ were considered statistically significant.

RESULTS

Capsaicin Upregulates TJ Expression in Rabbit SMG Cells

As the genes encoding the rabbit TJ molecules have not been reported, we designed primers from human TJ sequences.[7] Using cDNA from human SMG as positive controls, the mRNA expressions of ZO-1, Cldn-1, -2, -3, -4, -5, -7, and -11 were detectable in rabbit SMG (Figure 1a), whereas Cldn-6 was not detectable either in human or rabbit SMGs.

To investigate the effect of TRPV1 activation on the expression of TJ components, the primary cultured neonatal rabbit SMG cells were incubated with 10 μM capsaicin for the indicated times. The mRNA expressions of ZO-1 (Figure 1b), Cldn-3 (Figure 1c), and -11 (Figure 1d), but not Cldn-1, -2, -4, -5, and -7 (Supplementary Figure S1) were increased after capsaicin treatment for 12 h ($P < 0.01$) and 24 h ($P < 0.05$). Capsaicin incubation for 24 h also increased the protein levels of ZO-1, Cldn-3, and -11 (Figure 1e-g). In addition, pretreatment with 10 μM CPZ, an antagonist of TRPV1, abolished the capsaicin-induced increases in ZO-1, Cldn-3, and -11 mRNA expressions (Figure 1h-j), indicating capsaicin selectively upregulated expressions of TJ components through activation of TRPV1.

Capsaicin Increases TJ Permeability of Rabbit SMG

To explore the effect of TRPV1 activation on TJ function, the paracellular permeability assay was performed as described previously.[20] Two types of different molecular weight tracers (4 and 40 kDa FITC-dextrans) were used to monitor whether or not these tracers permeate into the acinar lumen across the TJ. Before capsaicin stimulation, the fluorescence was detectable in the basolateral space around each acinar islet, but rarely in the luminal space for 10 min. Figure 2a depicts that the fluorescence of 4 kDa FITC-dextran tracer (1 mg/ml) appeared in the acinar lumen from basolateral sides after capsaicin (10 μM) stimulation for 5 min (upper panel), and the quantitative analysis (lower panel) revealed that the fluorescent intensity in individual acini significantly increased after capsaicin treatment for 5 min. However, the paracellular permeability for a larger FITC-dextran (40 kDa, 1 mg/ml) was not affected by capsaicin (Figure 2b). Preincubation with CPZ (10 μM) abolished the capsaicin-induced 4 kDa FITC-dextran influx (Figure 2c), whereas the solvent DMSO alone did not induce the 4 kDa tracer influx (Figure 2d). These results indicated that capsaicin increased paracellular permeability for small macromolecules through activation of TRPV1.

Capsaicin Upregulates Expression of TJ Components in an ERK1/2-Dependent Manner

ERK1/2 is reported to be a crucial signal molecule that modulates the TJ expression and thereby affecting the paracellular transport in the Madin–Darby canine kidney (MDCK) and human intestinal T84 epithelial cells.[24–26] In cultured rabbit SMG cells, we found that p-ERK1/2 levels were rapidly increased by 55.8 and 59.6% after capsaicin incubation for 5 and 10 min, respectively ($P<0.01$), and returned to the basal level after 30 min, whereas total ERK1/2 was not changed (Figure 3a). After preincubation with PD98059 (20 μM), an ERK1/2 upstream kinase inhibitor, the capsaicin-induced increases in the mRNA expression of ZO-1, Cldn-3, and -11 were significantly

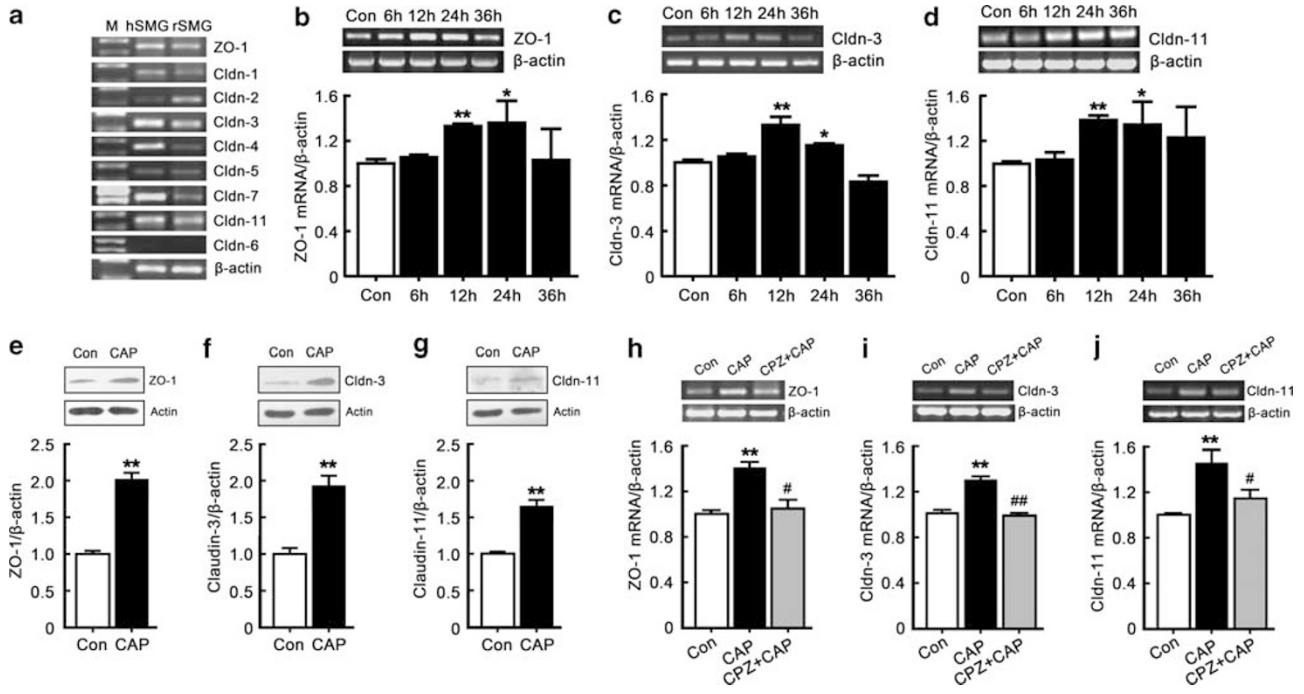

Figure 1 Effect of capsaicin on mRNA and protein expression of tight junction (TJ) components in rabbit submandibular gland (SMG) cells. (**a**) mRNA expressions of TJ components were detected by reverse transcription (RT)-PCR. (**b**–**d**) Time curve of zonula occludin-1 (ZO-1), claudin (Cldn)-3, and -11 mRNA expression induced by capsaicin. Cells were incubated with 10 μM capsaicin for 0–36 h. Expressions of ZO-1, Cldn-3, and -11 mRNA were normalized to those of β-actin. Values are means ± s.d. from three independent experiments performed in duplicate. $^{*}P<0.05$ and $^{**}P<0.01$ compared with Con. (**e**–**g**) Effect of capsaicin on ZO-1, Cldn-3, and -11 protein expression. Cells were incubated with 10 μM capsaicin for 24 h. The expressions of proteins were normalized to those of actin. Values are means ± s.d. from three independent experiments performed in duplicate. $^{**}P<0.01$ compared with Con. (**h**–**j**) The role of transient receptor potential vanilloid subtype 1 (TRPV1) in capsaicin-induced mRNA expressions of ZO-1, Cldn-3, and -11. Cells were pretreated with 10 μM capsazepine (CPZ) for 30 min. Values are means ± s.d. from three independent experiments performed in duplicate. $^{**}P<0.01$ compared with Con; $^{\#}P<0.05$ and $^{\#\#}P<0.01$ compared with CAP group. M, DNA marker; hSMG, human SMG; rSMG, rabbit SMG, Con, cells without capsaicin treatment, CAP, cells with capsaicin treatment for 24 h.

suppressed (Figure 3b–d), indicating that activation of ERK1/2 was required in capsaicin-mediated TJ expression. However, PD98059 pretreatment could not suppress the increased paracellular permeability of 4 kDa FITC-dextran induced by capsaicin (Figure 3e).

MLC2 Phosphorylation and F-actin Redistribution Are Related to Capsaicin-Mediated TJ Function

The MLC2 phosphorylation and reorganization of the cytoskeleton F-actin, the downstream molecules of MLC2, have been linked to enhance paracellular permeability of TJ in MDCK and Caco-2 cells or tissues.[27,28] Therefore, we explored the effects of capsaicin on MLC2 phosphorylation, as well as F-actin distribution in SMG. In primary cultured rabbit SMG cells, the level of p-MLC2 was significantly increased by 26.9 and 74.5% after capsaicin incubation for 5 and 10 min, respectively ($P<0.05$ and $P<0.01$, respectively; Figure 4a), and returned nearly to the basal level after 30 min, whereas total MLC2 was not changed.

To further explore the effect of MLC2 phosphorylation on capsaicin-induced TJ expression and function, rabbit SMG tissues or cells were pretreated with ML-7 (20 μM), an inhibitor of the MLC2 kinase. The capsaicin-induced increases in ZO-1, Cldn-3, and -11 expression were not inhibited (Figure 4b–d); however, the capsaicin-induced influx of 4 kDa FITC-dextran was abolished by ML-7 preincubation (Figure 4e). These results suggested that MLC2 phosphorylation was essential in capsaicin-induced increase in TJ permeability, but not in modulation of the TJ components' expressions.

Under unstimulated conditions, F-actin was mostly localized in the cytoplasm of the primary cultured neonatal rabbit SMG cells (Figure 5a). Capsaicin incubation for 5 and 10 min significantly increased the fluorescence intensity of F-actin in peripheral cell membrane, which was suppressed by preincubation with CPZ or ML-7, but not PD98059 (Figure 5a). Quantitative analysis showed that the fluorescent intensity of F-actin in the perimembrane after treatment with capsaicin for 5 and 10 min was significantly higher than that of controls (1.68 ± 0.40 and 1.00 ± 0.22 for CAP 5 min and Con, respectively, $P<0.01$; 1.58 ± 0.11 and 1.00 ± 0.22 for CAP 10 min and Con, respectively, $P<0.05$; Figure 5b), whereas it was inhibited by preincubation with CPZ (0.91 ± 0.23) and ML-7 (1.07 ± 0.20), but not PD98059 (1.41 ± 0.06). The ratio of F-actin in perimembrane to total F-actin was also significantly increased in capsaicin-treated

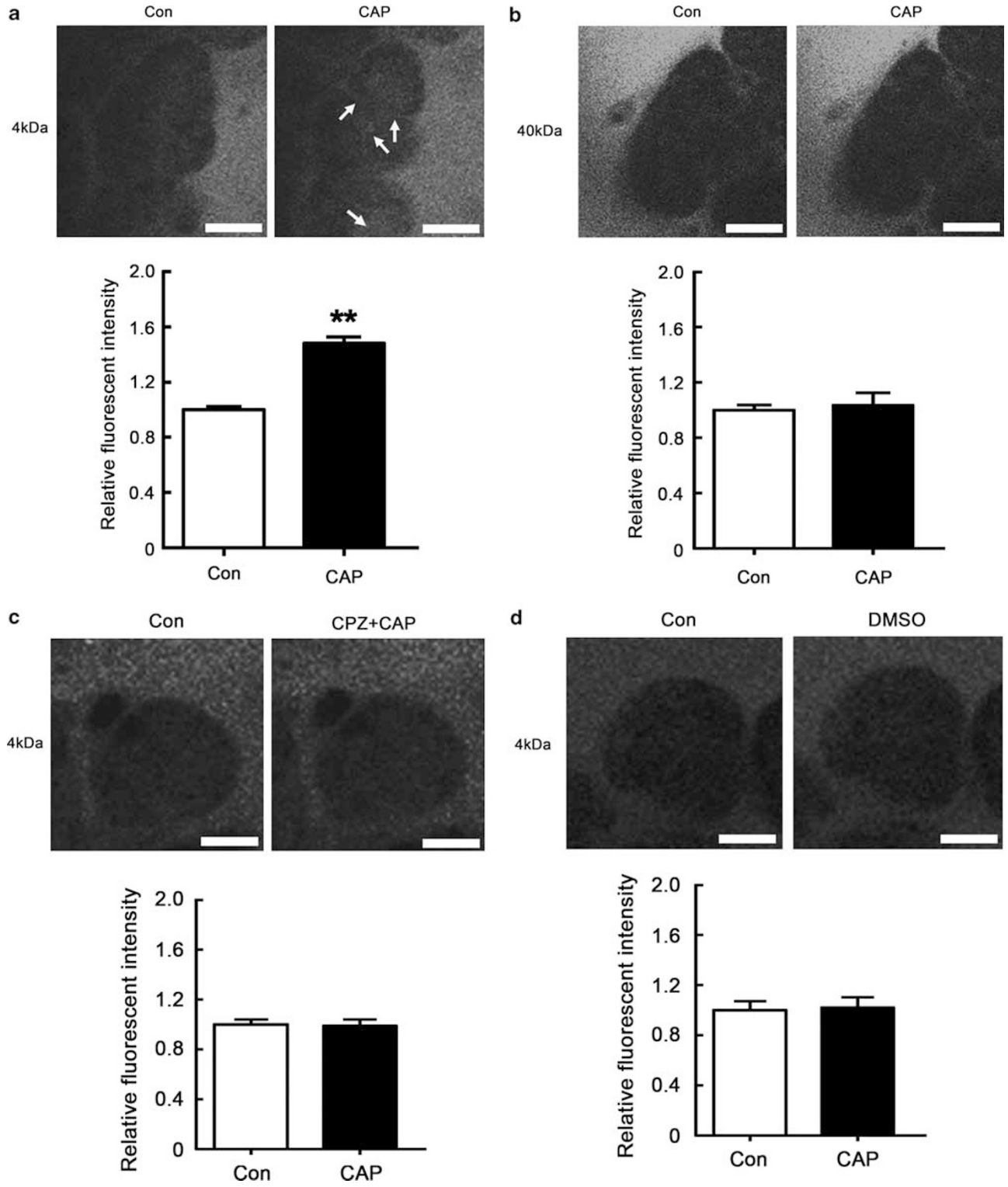

Figure 2 Effect of capsaicin on tight junction (TJ) permeability in submandibular gland (SMG) tissues. Rabbit SMGs were cut into small pieces, and paracellular permeability assay using 4 kDa and 40 kDa FITC-dextrans (1 mg/ml, green), as paracellular tracers was performed under confocal microscopy. (**a**) The influx of 4 kDa FITC-dextran induced by 10 μM capsaicin stimulation. (**b**) The influx of 40 kDa FITC-dextran induced by capsaicin. (**c**) The role of transient receptor potential vanilloid subtype 1 (TRPV1) in capsaicin-induced influx of 4 kDa FITC-dextran. Tissues were pretreated with 10 μM capsazepine (CPZ). (**d**) The influx of 4 kDa FITC-dextran induced by the solvent dimethyl sulfoxide (DMSO) alone. Upper panel: the fluorescence images before (Con) and after 10 μM capsaicin stimulation in normal SMG tissues (CAP), tissues with CPZ pretreatment (CPZ + CAP) and DMSO alone (DMSO) at 300 s; lower panel: quantitative analysis representing the fluorescent intensity within individual acini at 300 s. Arrows (white) denote the entering of fluorescence tracer into the acinar lumen after capsaicin stimulation. Each image and column is a representative of three separate experiments. $^{**}P<0.01$ compared with Con. Scale bar represents 10 μm.

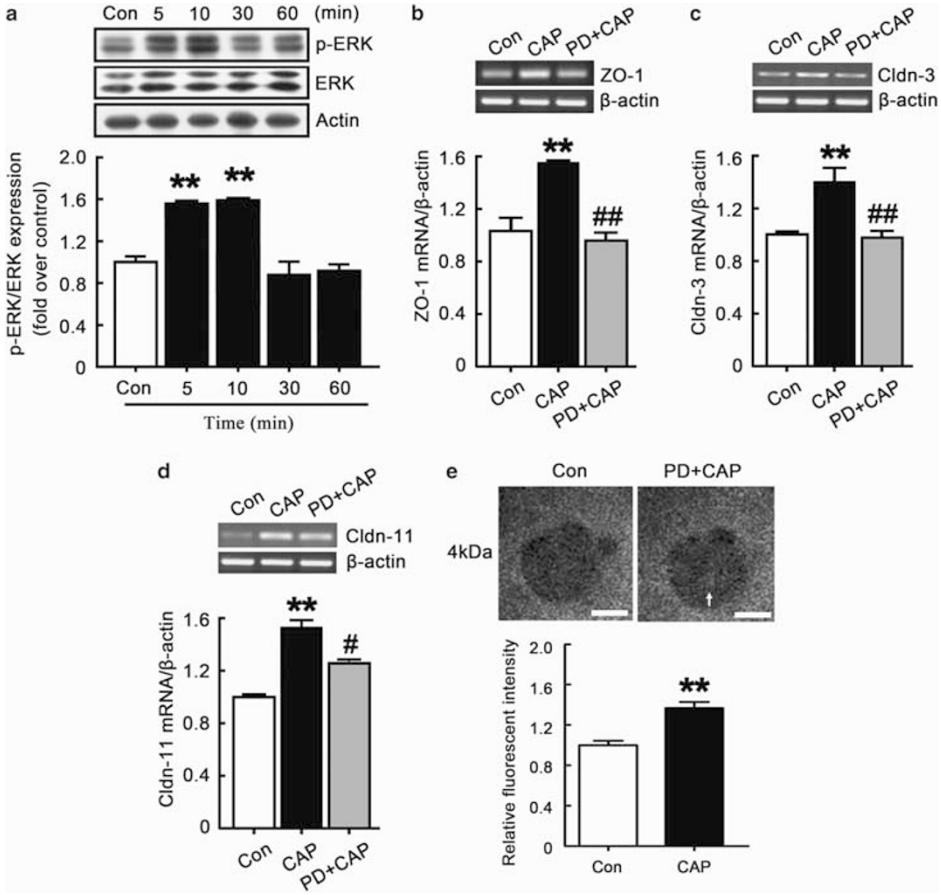

Figure 3 Effect of extracellular signal-regulated kinase 1/2 (ERK1/2) on capsaicin-induced tight junction (TJ) components' expression, and TJ permeability in submandibular gland (SMG) cells and tissues. Rabbit SMG cells were treated with 10 μM capsaicin for 0–60 min. (**a**) Time curve of phosphorylation of ERK1/2 (phospho-ERK1/2 (p-ERK1/2)). The levels of p-ERK1/2 were normalized to total ERK1/2. Values are means ± s.d. from three independent experiments performed in duplicate. $^{**}P<0.01$ compared with Con. (**b**–**d**) Effect of ERK1/2 on capsaicin-induced zonula occludin-1 (ZO-1), claudin (Cldn)-3, and -11 mRNA expressions. Cells were preincubated with an ERK1/2 upstream kinase inhibitor, PD98059 (PD; 20 μM) for 30 min. Expressions of ZO-1, Cldn-3, and -11 mRNA were normalized to those of β-actin. Values are means ± s.d. from three independent experiments performed in duplicate. $^{**}P<0.01$ compared with Con; $^{\#}P<0.05$, and $^{\#\#}P<0.01$ compared with CAP group. (**e**) Effect of ERK1/2 on capsaicin-induced TJ permeability by using the 4 kDa FITC-dextran (1 mg/ml). SMG tissues were preincubated with 20 μM PD98059 (PD). Upper panel: the fluorescence images before (Con) and after PD98059 preincubation followed by capsaicin treatment (PD + CAP); lower panel: quantitative analysis representing the fluorescent intensity within individual acini at 300 s. Arrow (white) denotes the entering of fluorescence tracer into the acinar lumen. Each image and column is a representative of three separate experiments. Scale bar represents 10 μm.

cells for 5 and 10 min, whereas it was suppressed by pre-incubation with CPZ and ML-7, but not with PD98059 (Figure 5c). The results suggested that capsaicin induced F-actin redistribution from cytoplasm to peripheral cell membrane through TRPV1 activation, and MLC2, but not ERK1/2, was required in capsaicin-mediated F-actin redistribution.

Capsaicin Increases Saliva Secretion of Transplanted Glands

The basal saliva flow rate among control, transplanted, and capsaicin groups before transplantation showed no difference (Table 2). Saliva secreted from the transplanted SMGs decreased significantly on postoperative day 2 and was barely detectable on days 4 and 7. Topical capsaicin cream (0.2 g, with 0.075% capsaicin, twice per day) applied to the skin covering the transplanted SMGs considerably increased the secretion of the transplanted glands ($P<$ 0.01; Table 2).

Capsaicin Diminishes the TJ Structural Injury of Transplanted Glands

In control glands, TJs located in the most apical portion between neighboring epithelial cells and formed a slightly dilated distance under transmitted electron microscope, whereas in transplanted glands, the width of apical TJs was significantly reduced and TJ structure was not as vivid as normal, as visualized by a lower electron-dense and a less-defined architecture in the apical portion, indicating a structural injury occurred in the transplanted SMGs (low- and high-magnification micrographs in upper and lower panels, Figure 6a). The alteration in TJ ultrastructure in the

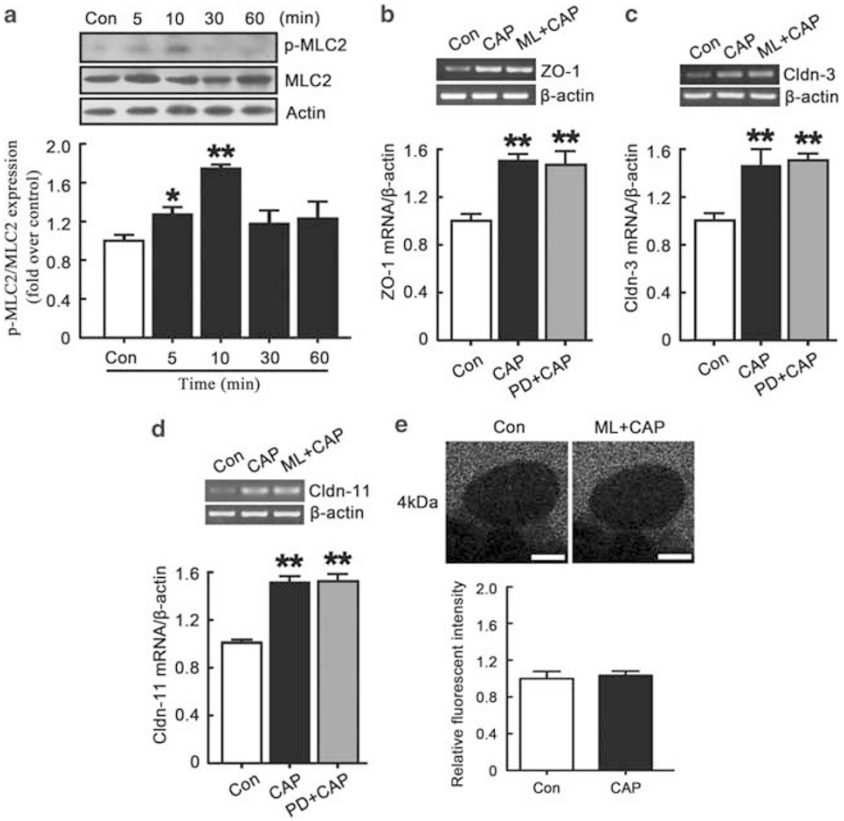

Figure 4 Effect of myosin light chain 2 (MLC2) on capsaicin-induced tight junction (TJ) components' expression, and TJ permeability in submandibular gland (SMG) cells and tissues. Rabbit SMG cells were treated with 10 μM capsaicin for 0–60 min. (**a**) Time curve of phosphorylation of MLC2 (phospho-MLC2 (p-MLC2)). The levels of p-MLC2 were normalized to total MLC2. Values are means ± s.d. from three independent experiments performed in duplicate. $^{*}P<0.05$ and $^{**}P<0.01$ compared with Con. (**b**–**d**) Effect of MLC2 on capsaicin-induced zonula occludin-1 (ZO-1), claudin (Cldn)-3, and -11 mRNA expressions. Cells were preincubated with an inhibitor of MLC2 upstream kinase, ML-7 (ML; 20 μM) for 30 min. Expressions of ZO-1, Cldn-3, and -11 mRNA were normalized to those of β-actin. Values are means ± s.d. from three independent experiments performed in duplicate. $^{**}P<0.01$ compared with Con. (**e**) Effect of MLC2 on capsaicin-induced TJ permeability by using the 4 kDa FITC-dextran (1 mg/ml). SMG tissues were preincubated with 20 μM ML-7 (ML). Upper panel: the fluorescence images before (Con) and after ML-7 preincubation followed by capsaicin treatment (ML + CAP); lower panel: quantitative analysis representing the fluorescent intensity within individual acini at 300 s. Each image and column is a representative of three separate experiments. Scale bar represents 10 μm.

transplanted SMGs was reversible by capsaicin treatment for 7 days, which showed similar structure to those of controls. However, the ultrastructure of adherens junction (AJ), another junctional complex of epithelium located just basal to TJ, was unchanged among the three groups (shown as 'AJ' in Figure 6a). The proportion of low-matrix-density secretory granules was more reduced in transplanted glands than in controls (shown as 'G' in Figure 6a), whereas abundant but smaller secretory granules were seen after capsaicin treatment, which were in accordance with the previous study.[19] Morphometric assessment of TJs revealed that the average width of apical TJs was 10.73 ± 0.31 nm in control glands (Figure 6b). However, the TJ width in transplanted glands was significantly more reduced than that of the controls (3.67 ± 0.74 nm, $P<0.01$), whereas it was recovered after capsaicin treatment (10.69 ± 1.19 nm). These results indicated that the structural injury of TJs might be involved in hyposecretion of the transplanted SMGs and capsaicin could diminish TJ structural injury of the transplanted glands.

Capsaicin Increases TJ Components Expression in Transplanted Glands

The mRNA expressions of ZO-1, Cldn-3, and -11 were decreased by 18.1, 44.4, and 53.0%, respectively, in the transplanted glands compared with those of controls ($P<0.05$; Figure 7a–c), whereas the mRNA expression levels of these TJ molecules were close to the control levels after capsaicin treatment. The protein levels of ZO-1, Cldn-3, and -11 were also significantly decreased by 18.7, 25.1, and 46.1%, respectively. Capsaicin increased the protein levels of these three TJ components after transplantation ($P<0.05$; Figure 7d–f). Expression of mRNA levels of other TJ molecules, including Cldn-1, -2, -4, -5, -7, and -11 were not significantly changed among the three groups (Supplementary Figure S2).

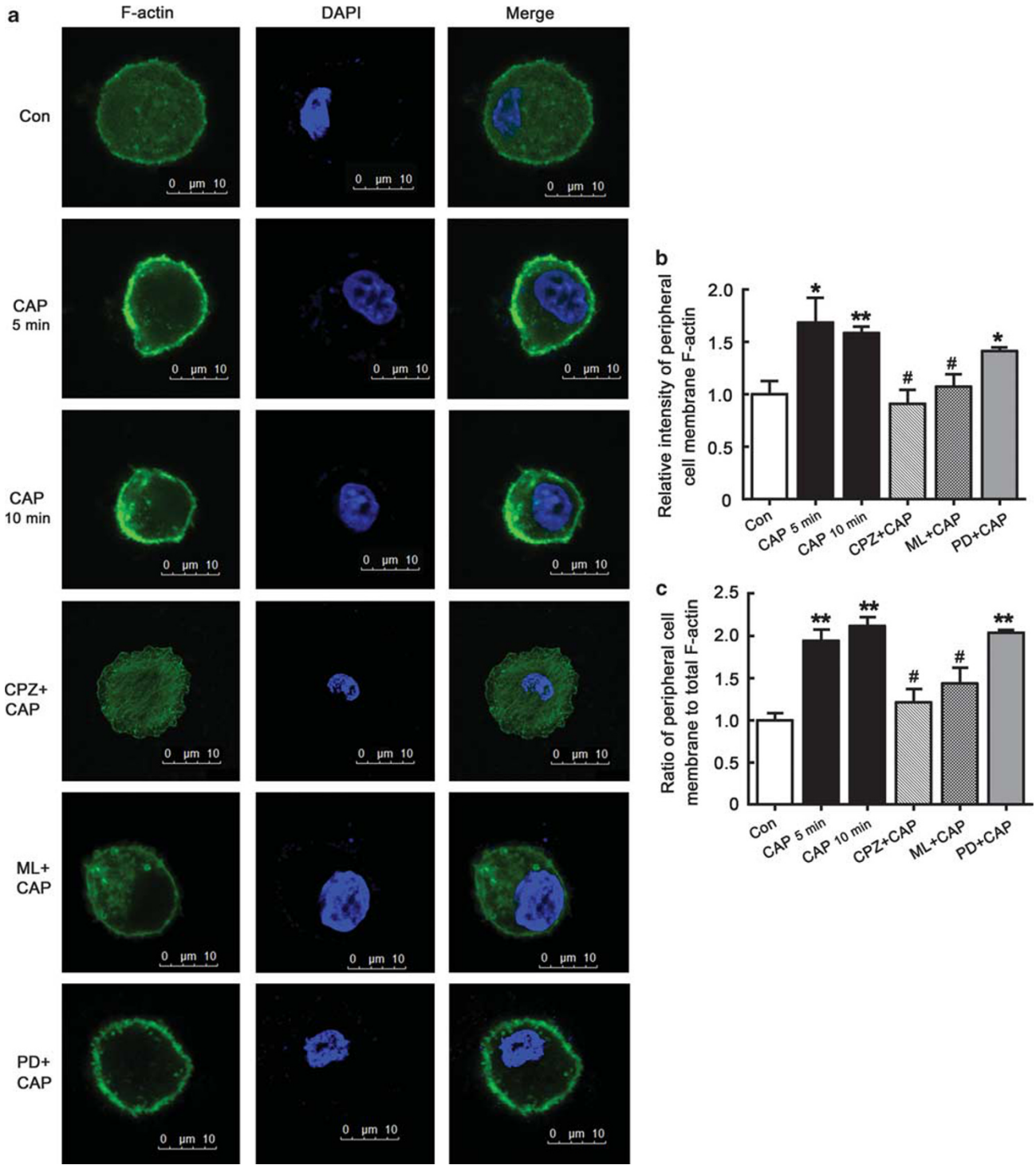

Figure 5 (**a**) Effect of myosin light chain 2 (MLC2) and extracellular signal-regulated kinase 1/2 (ERK1/2) on capsaicin-induced F-actin distribution in submandibular gland (SMG) cells. Cells were treated with 10 μM capsaicin for 5 min (CAP 5 min) and 10 min (CAP 10 min). Preincubation with capsazepine (CPZ) (CPZ + CAP), ML-7 (ML + CAP), and PD98059 (PD + CAP) were also performed to evaluate the role of transient receptor potential vanilloid subtype 1 (TRPV1), MLC2, and ERK1/2 in capsaicin-induced F-actin distribution. Cells were labeled with FITC-labeled phalloidin (green), and nuclei were labeled with DAPI (4′,6-diamidino-2-phenylindole; blue). Scale bar represents 10 μm. (**b**) The fluorescence of F-actin in peripheral cell membrane in Con, CAP 5 min, CAP 10 min, CPZ + CAP, ML + CAP, and PD + CAP groups was measured from 10 randomly fields. Values are means ± s.d. from three independent experiments performed in duplicate. $^{*}P<0.01$ and $^{**}P<0.01$ compared with Con; $^{\#}P<0.05$ compared with CAP 5 min. (**c**) The ratio of F-actin in peripheral cell membrane to total was measured from 10 randomly fields. Values are means ± s.d. from three independent experiments performed in duplicate. $^{**}P<0.01$ compared with Con; $^{\#}P<0.05$ compared with CAP 5 min.

The immunostaining of ZO-1 was also performed to demonstrate its change at the protein level. In control glands, ZO-1 was expressed principally at the apical-most portion of the lateral membrane (Figure 7g, upper panel). After transplantation, an obvious reduced immunofluorescence intensity of ZO-1 at the most apical portion was seen, whereas ZO-1 was reexpressed at the apical-most area similar to normal in capsaicin-treated glands. Similar alterations in Cldn-3 distribution were also seen among three groups (Figure 7g, middle panel). However, the distribution of Cldn-4, which showed a stronger staining in ducts than in acini, was unchanged in either transplanted or capsaicin-treated glands (Figure 7g, lower panel).

Table 2 Effects of capsaicin on saliva secretion in transplanted SMGs

	Saliva secretion (mm/5 min)		
Postoperative day	Con	T	T+CAP
0	5.8 ± 0.76	6.3 ± 0.91	6.7 ± 0.97
2	6.0 ± 0.82	2.5 ± 0.76*	9.1 ± 1.10$^{*,\ ***}$
4	6.3 ± 0.91	0.6 ± 0.07**	12.1 ± 2.03$^{*,\ ***}$
7	6.7 ± 0.97	0.5 ± 0.08**	12.4 ± 2.04$^{*,\ ***}$

Abbreviations: Con, control; SMG, submandibular gland; T, transplanted; T+CAP, transplanted with capsaicin treatment.
Data are means ± s.d. Capsaicin cream (0.2 g, with 0.075% capsaicin, twice per day) was applied to the skin covering the transplanted SMGs. Saliva secretion was measured for 5 min by the moistened length of filter paper (35 × 5 mm) through the cannula inserted into the Wharton's duct, and collected before (postoperative day 0) or after the transplantation (postoperative days 2, 4 and 7). $^{*}P<0.05$ and $^{**}P<0.01$ compared with the baseline (Con) for each column. $^{***}P<0.01$ compared with T. $n=4$ per group.

Capsaicin Recovers F-actin Morphology in Transplanted Glands

In addition, we evaluated the effects of capsaicin on F-actin morphology of SMG *in vivo*. Under confocal microscopy, the intense staining of F-actin was shown in the peri-apicolateral region of control SMGs, whereas the fluorescent intensity of these regions was significantly diminished in transplanted SMGs. After capsaicin treatment for 7 days, the fluorescent intensity of F-actin was increased and was mostly relocated to peri-apicolateral membrane regions of acini (Figure 8a). Quantitative analysis showed that the fluorescent intensity of peri-apicolateral F-actin in transplanted glands was significantly lower than that of controls (0.57 ± 0.07 *vs* 1.00 ± 0.19, $P<$ 0.05; Figure 8b), whereas it recovered to normal in capsaicin-treated glands (1.05 ± 0.13). The ratio of F-actin in peri-apicolateral regions to total F-actin of each acinus in transplanted glands reduced by 29.4% compared

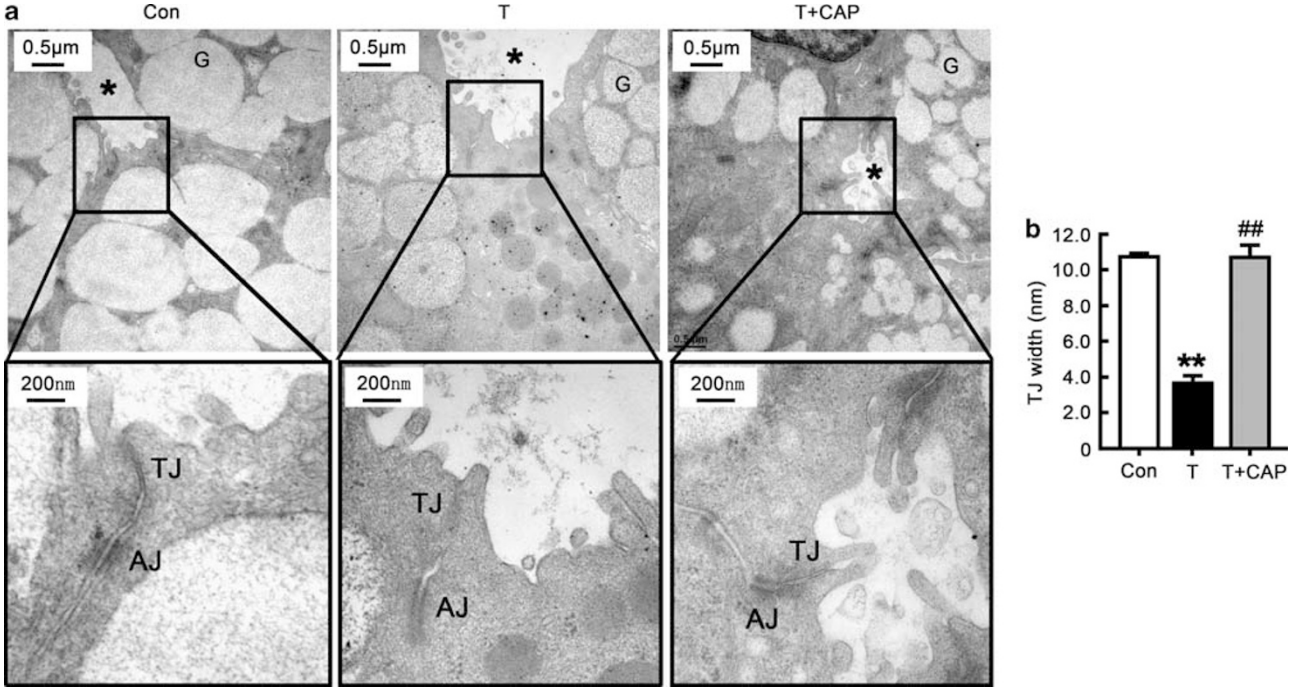

Figure 6 Effect of capsaicin on tight junction (TJ) ultrastructure in submandibular glands (SMGs). The transplanted glands were removed on postoperative day 7, and observed under transmitted electron microscope. (**a**) Representative TJ ultrastructure images of control glands (Con), transplanted glands (T), and transplanted with capsaicin treatment glands (T + CAP). Upper panel: bars indicate 0.5 μm; lower panel: the higher magnification of the TJ regions with bars indicating 200 nm. (**b**) The width of apical TJs was measured from 5 sections of 10 random fields in each section among Con, T, and T + CAP groups. $^{**}P<0.01$ compared with Con; $^{\#\#}P<0.01$ compared with T. * Shows acinar lumen; G, low-matrix-density secretory granule; AJ, adherens junction.

with that in controls ($P< 0.05$; Figure 8c), whereas it was increased in the capsaicin-treated group ($P< 0.05$; Figure 8c). These results suggested that F-actin disruption might be involved in the hypofunction of the transplanted glands, and capsaicin-induced SMG secretion involved the modulation of F-actin distribution *in vivo*.

DISCUSSION

In this study, we provided the first evidence that TRPV1 activation in SMG not only selectively upregulated the expression of ZO-1, Cldn-3, and -11 in an ERK1/2-dependent manner, but also induced an increase in TJ permeability and F-actin redistribution via activation of MLC2. Furthermore, in a hyposecretory model with rabbit SMG transplantation, topical capsaicin treatment significantly increased the secretion, protected the TJ structure against destruction, reversed the decreased ZO-1, Cldn-3, and -11 levels, and recovered F-actin distribution in transplanted SMGs. Accordingly, these results suggest that TJ components, particularly ZO-1, Cldn-3, and -11, are of vital importance to SMG secretion under both physiological and pathophysiological conditions. Hyposecretion in the transplanted SMGs involved the alteration of TJ expression, function, and structure, and TRPV1 might be a potential target to improve saliva secretion through mediating TJ integrity.

It is well-known that water, ion, and solute transport across an epithelial cell layer can be via either transcellular or paracellular route.[1,2] To date, most studies referring to the SMG secretion focus on the transcellular route through aquaporin channels,[14,15,29] whereas only a few studies focus on the paracellular pathway.[30,31] As the basic structure of the paracellular pathway, TJ is a multi-protein complex consisting of transmembrane proteins and intracellular scaffold proteins. However, the composition of TJ varies among different types of cells, tissues, and species.[1,2] Previous studies have demonstrated that ZO-1, Cldn-1 to -5, -7, and -11 are expressed in human major salivary glands,[7] ZO-1, Cldn-1, -3, -4, -5, and occludin in rat salivary tissue,[8,9] and ZO-1, Cldn-3 to -8, -10, and -11 in mouse SMG.[10,11] Here we provided further evidence that ZO-1, Cldn-1, -2, -3, -4, -5, -7, and -11 exist in rabbit SMGs, indicating that the expression pattern of TJ components was much closer between rabbit and human SMG.

TRPV1 was originally found only in neural cells; however, much attention has recently focused on the non-neural expression of TRPV1.[32–34] We previously demonstrated a functional TRPV1 in human and rabbit SMGs, and that the TRPV1-induced salivation involves, at least in part, the modulation of AQP5 expression and distribution.[14,15] However, according to some recent studies, in addition to the

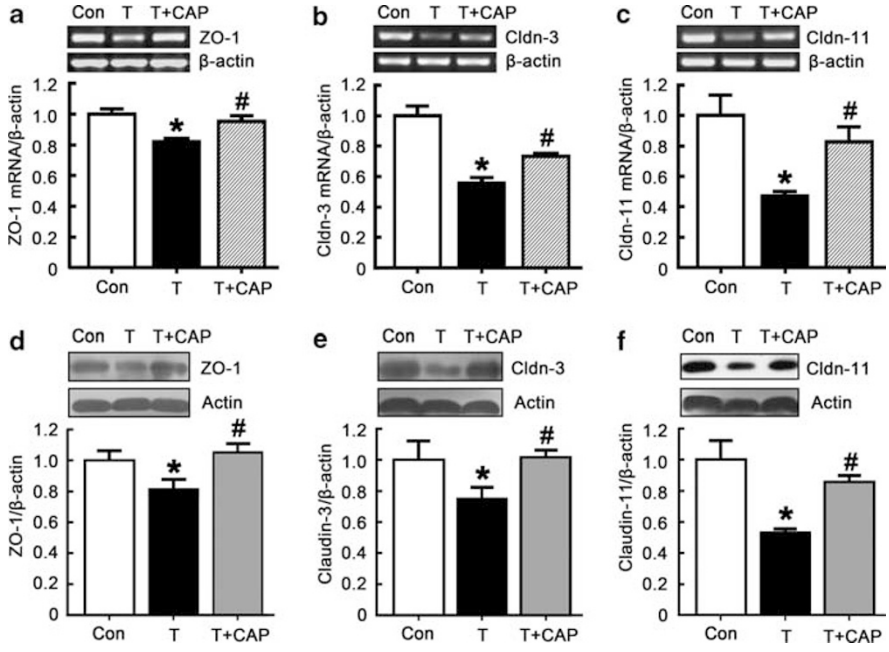

Figure 7 Effect of capsaicin on mRNA and protein expression of zonula occludin-1 (ZO-1), claudin (Cldn)-3, and -11 and distribution of ZO-1 and Cldn-3 in submandibular glands (SMGs). The transplanted glands were harvested on postoperative day 7. (**a**–**c**) Effect of capsaicin on ZO-1, Cldn-3, and -11 mRNA expression. The levels of ZO-1, Cldn-3, and -11 mRNA were normalized to those of β-actin. Values are means ± s.d. from three independent experiments performed in duplicate. $^{*}P<0.05$ compared with Con; $^{\#}P<0.05$ compared with T. (**d**–**f**) Effect of capsaicin on ZO-1, Cldn-3, and -11 protein expression. The levels of ZO-1, Cldn-3, and -11 protein were normalized to those of actin. Values are means ± s.d. from three independent experiments performed in duplicate. $^{*}P<0.05$ compared with Con; $^{\#}P<0.05$ compared with T. (**g**) Effect of capsaicin on ZO-1 (upper panel), Cldn-3 (middle panel), and Cldn-4 (lower panel) distribution among Con, T and T + CAP groups. Each image is a representative of three separate experiments. Upper and middle panels: bars indicate 5 μm; lower panel: bars indicating 20 μm. Each image is a representative of three separate experiments.

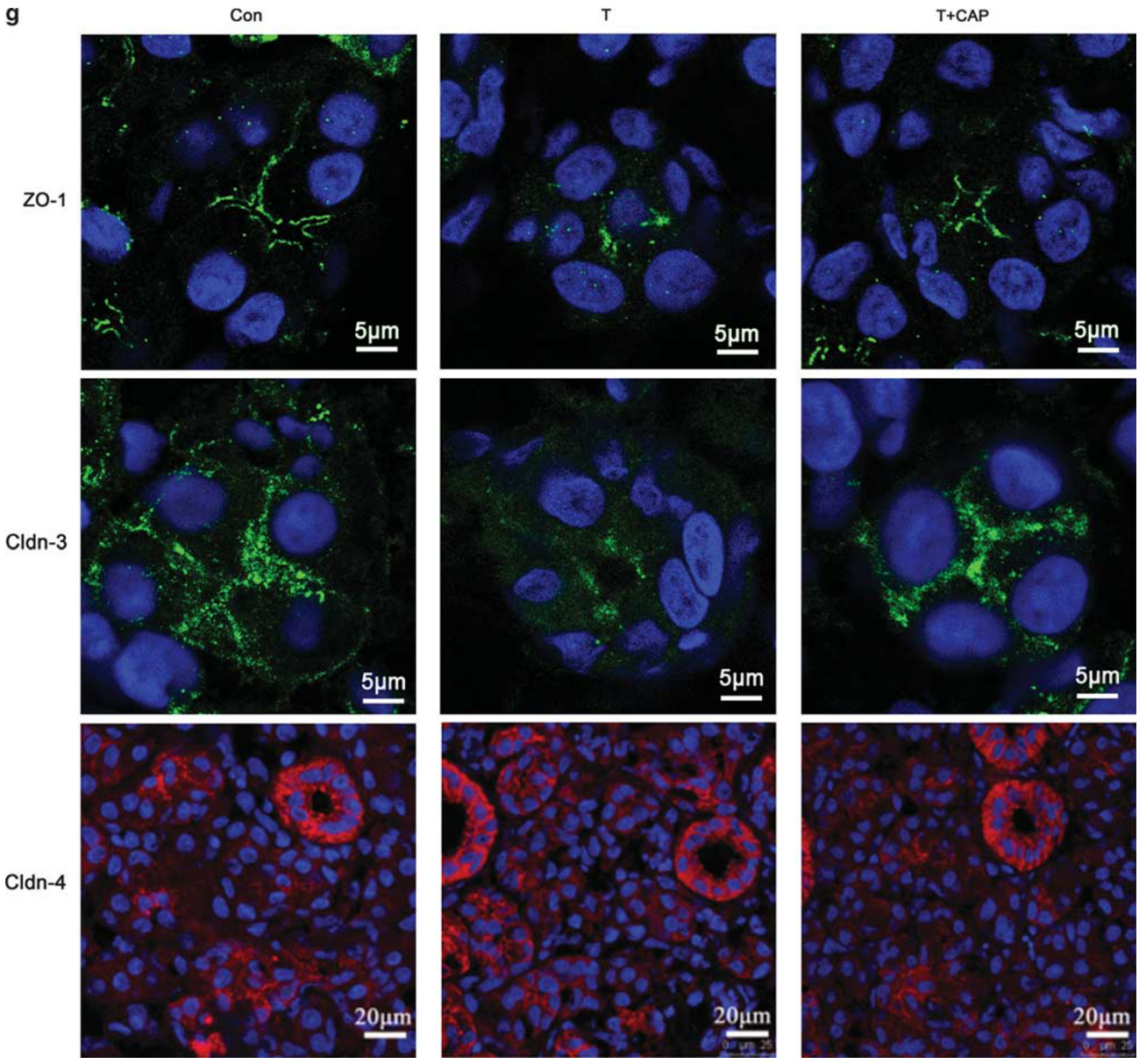

Figure 7 Continued.

aquaporin 5-mediated transcellular route, the saliva secretion induced by the agonists of muscarinic receptor and adrenoceptor, such as carbachol and isoproterenol, also involves the modulation of TJs, resulting in significantly increased paracellular transport.[20,30,31] Thus, the TJ-mediated parcellular route has gained much attention regarding its potential role in salivary secretion. Although capsaicin was reported to increase TJ paracellular permeability in intestinal Caco-2 cells,[16] the activation of TRPV1 on TJ properties of SMG is still unknown. The present study demonstrated that capsaicin increased the mRNA and protein expressions of ZO-1, Cldn-3, and -11, but not Cldn-1, -2, -4, -5, and -7 in cultured SMG cells. In addition, the increased expressions of these TJ components were abolished by the pretreatment of CPZ, indicating that activation of TRPV1 by capsaicin selectively upregulated salivary TJ molecules at the transcriptional level.

As an integral complex, the expression level of each TJ component contributes to the TJ structural integrity and paracellular permeability under both physiological and pathological conditions. In rat parotid gland Par-C10 cells, the proinflammatory cytokines tumor necrosis factor-α (TNF-α) and/or interferon-γ (IFN-γ) causes a reduced expression of Cldn-1, but not Cldn-3, -4, -10, ZO-1, JAM-1, and occludin, which was associated with the decrease in transepithelial resistance and anion secretion.[35] In a hyposecretion model using AQP5 knockout mice, the protein expressions of Cldn-3, -7, and occludin are found signi-

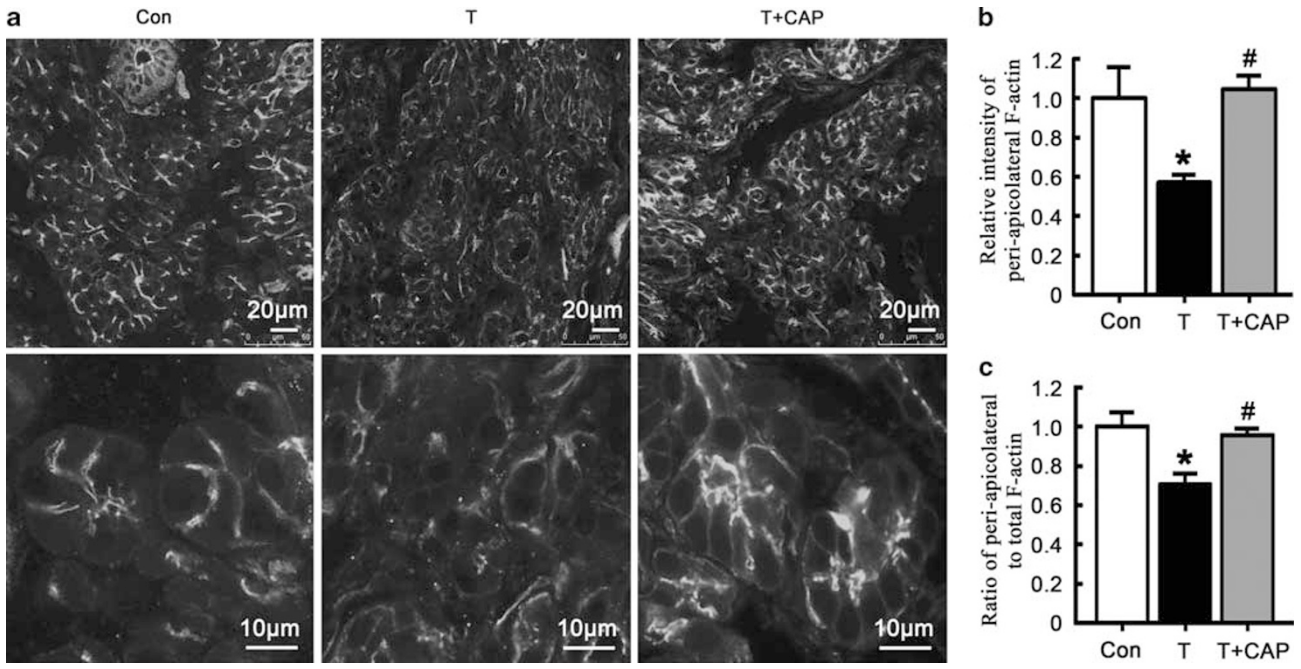

Figure 8 Effect of capsaicin on F-actin morphology in submandibular glands (SMGs). The transplanted glands were harvested on postoperative day 7. Sections (6 μm) were labeled with FITC-phalloidin (green), and examined by confocal microscopy. (**a**) Representative immunofluorescence images of F-actin in control (Con), transplanted (T), and transplanted with capsaicin-treated glands (T + CAP). Upper panel: bars indicate 20 μm; lower panel: the higher magnification of the acini with bars indicating 10 μm. (**b**) The fluorescence of F-actin in peri-apicolateral region of acini in Con, T, and T + CAP groups was measured from 5 sections of 10 random fields in each section. $^{*}P<0.05$ compared with Con; $^{\#}P<0.05$ compared with T. (**c**) The ratio of F-actin in peri-apicolateral region to total F-actin of each acinus was measured from 5 sections of 10 random fields in each section. $^{*}P<0.05$ compared with Con; $^{\#}P<0.05$ compared with T.

ficantly decreased along with a reduced paracellular permeability in mouse parotid.[36] Another recent study in the labial salivary glands from Sjõgren's syndrome patients showed that ZO-1 is downregulated, whereas Cldn-1 and -4 were upexpressed.[37] These findings suggest that the exact role of each TJ molecule may vary, depending on the cells, tissue, species investigated, and the cause of disease. ZO-1 is an important intracellular scaffold protein that links the transmembrane TJ proteins with actin cytoskeleton.[1,2] Increased expression of ZO-1 is found to be associated with decreased paracellular permeability in the corneal and retinal pigment epithelium,[38,39] whereas the absence of ZO-1 results in a slight delay in the formation of TJ in MDCK cells and mouse mammary epithelial cells.[40] In MDCK I cells, the expression of Cldn-3 is not related with paracellular permeability,[41] whereas in gastric polarized epithelial cell line (MKN28), the knockdown expression of Cldn-3 induces a significant increase in paracellular permeability.[42] Cldn-11 is reported to be involved in nerve conduction, spermatogenesis, and stria vascularis function.[43–45] Although ZO-1, Cldn-3, and -11 have already been detected in human and mouse SMGs, their functions in saliva secretion are still unknown. In the present study, we showed that the decreased expression of ZO-1, Cldn-3, and -11 in transplanted rabbit SMGs was associated with hyposecretion, and capsaicin significantly promoted the saliva secretion and increased levels of ZO-1, Cldn-3, and -11 *in vivo* and *in vitro*. These results together suggested that ZO-1, Cldn-3, and -11 might have a critical role in the saliva secretion of SMG, particularly in maintaining TJ integrity, and the decrease or lack of these TJ components could reduce paracellular transport and lead to hyposecretion of rabbit SMG. TRPV1 activation by capsaicin promoted secretion of normal and hypofunctional SMGs partly by upregulating ZO-1, Cldn-3, and -11 expressions. Moreover, by using immunofluorescence staining, we showed that capsaicin treatment ameliorated the decreased expression of ZO-1 and Cldn-3 at the most apical portion of the cell–cell interaction in the transplanted hypofunctional SMGs, whereas the level and localization of Cldn-4 were unchanged among three groups. The changes in the distribution of ZO-1, Cldn-3, and -4 were in accordance with their expression levels in transplanted and capsaicin-treated glands, which provided further evidence that capsaicin treatment was able to modulate both the expression and distribution of specific TJs in parallel, in rabbit SMGs. However, the attempts to display the distribution of Cldn-11, as well as the other unchanged components like Cldn-1, remained unsuccessful due to the inappropriate commercial immunostaining antibodies against these TJ components in rabbit tissues. Therefore, further efforts should be made as to fully demonstrate that capsaicin-induced TJ changes were specific and not globally disrupted.

The function of TJ is usually evaluated by the paracellular permeability assay for different weight fluorescence tracers. Isoproterenol induces 40 kDa FITC-dextran to enter the luminal space, whereas carbachol only induces 10 kDa tracer influx in rat parotid and SMG, indicating β-adrenoceptor activation causes more dilated opening of TJ permeability than muscarinic cholinergic receptor activation.[20] Here we showed that capsaicin caused the 4 kDa FITC-dextran, but not the 40 kDa FITC-dextran, entering into acinar lumen and this influx was abolished by CPZ. These results further indicated that activation of TRPV1 not only selectively increased expression of the TJ molecules, but also regulated the TJ function by increasing paracellular permeability for small macromolecules in rabbit SMG.

In addition to the detection of TRPV1-induced TJ expression and paracellular permeability, the TJ ultrastructure under transmitted electron microscopy was directly visualized in the transplanted hypofunctional SMGs. Previous studies reported that exposure to sodium caprate and pathological stimuli in Caco-2 cells results in structural alterations of TJ with a form of dilations, which is in parallel with enhanced paracellular permeability.[46] Another study in mouse intestine mucosa showed that the normal TJ width, which represents the distance between neighboring cells, is 13.84 ± 1.04 nm, whereas it is reduced by 50% in ClC-$2^{-/-}$ mouse intestine (6.8 ± 0.33 nm), in parallel with a significantly decreased paracellular permeability.[23] Accordingly, the TJ width, to some extent, can act as an indicator of normal or abnormal TJ structure. It has been reported that the AJ in mouse SMG is 10–15 nm, which suggests that the TJ width should be less than that.[47] However, no data referring to TJ width in rabbit SMG has been shown yet. Here we observed a slightly dilated distance between neighboring TJs in normal rabbit SMGs, and the morphometric assessment of the TJs revealed that the TJ width was 10.73 ± 0.31 nm, indicating that TJ must open up normally to allow material transport into the acinar lumen via paracellular transport. However, the width of apical TJs significantly reduced with a less invalid structure of TJs, indicating an ultrastructural injury occurring in the transplanted SMGs. These changes in TJs appear to be responsible for the altered secretory function in transplanted glands. After capsaicin treatment, TJ structural integrity was recovered. These observations provided visualized evidence that TJ structure was critical for maintaining SMG secretion. The changes in TJ ultrastructure were also in accordance with our results that showed a decreased and a reversed expression and function of TJs in transplanted and capsaicin-treated SMGs. These results further supported the possibility that the functional and structural alteration in TJs might be a primary or contributing reason for hyposecretion of the transplanted SMGs, and capsaicin promoted saliva secretion probably by diminishing TJ structural and functional injury of the transplanted glands.

We further explored the signal molecules linking TRPV1 activation to TJ expression and function. ERK1/2 has an important role in modulating paracellular transport by up- or downregulating the TJ expression. In MDCK cells, ERK1/2 activation by TNF-α and IFN-γ triggers the loss of Cldn-2 mRNA expression,[24] whereas TGF-β upregulates the mRNA expression of Cldn-1 and ZO-2 through ERK1/2 activation.[25] In human colon T84 cells, the activation of ERK1/2 was also involved in the interleukin-17-induced increased expression of Cldn-1 and -2.[26] The present study showed that in rabbit SMG cells, ERK1/2 was phosphorylated by capsaicin, and preincubation with ERK1/2 kinase inhibitor PD98059 suppressed the increased expressions of ZO-1, Cldn-3, and -11, but did not affect the capsaicin-induced increase in small macromolecule entering into the acinar lumen. These results indicated that the activated ERK1/2 was involved in capsaicin-induced TJ expressions, but not TJ permeability. However, the detailed regulatory mechanism involved in the ERK1/2-dependent TJ expressions in rabbit SMGs is still unknown. In MDCK cells, epidermal growth factor activates ERK1/2 pathways and increases Sp1 expression, resulting in an elevation of Cldn-4 expression.[48] Several other transcriptional factors, such as Jun, Fos, C/EBP, the zinc-finger transcription factor Snail, and the Ets family transcription factor ELF3 are also reported to be associated with the regulation of specific TJ expressions,[49–51] but the effects of activated ERK on these transcription factors are unclear. Further studies addressing these issues are in progress at our laboratory.

The intracellular pathway connecting activation of TRPV1 to increased TJ permeability remains unclear, but one important molecule may be MLC2, which is a member of the regulatory light chains of the motor protein myosin II. Previous studies indicated that increased TJ permeability triggered by pathogenic treatment with TNF-α, IFN-γ, or bile acids involves the phosphorylation of MLC2.[52,53] Some cellular transporters also affect the TJ function by activating MLC2. The permeability of intestinal TJ is increased through a MLC2-dependent pathway after transfection with Na^+-glucose cotransporter (SGLT1) in Caco-2 cells.[54] Further study showed that inhibition of sodium hydrogen exchange, another important cellular transporter, induces decreases in both TJ permeability and MLC2 phosphorylation in Caco-2 cells with active SGLT1, indicating that sodium hydrogen participates in SGLT1-regulated TJ function via the MLC2-signaling pathway.[55] These studies altogether demonstrate that both exogenous stimuli and intracellular transporters regulate TJ function through a shared MLC2 pathway. Interestingly, a recent study pointed out that MLC2 phosphorylation alone is sufficient to modulate TJ function.[27] In the present study, we demonstrated that capsaicin increased MLC2 phosphorylation in rabbit SMG cells, and the activated MLC2 contributed to capsaicin-induced TJ permeability. These results indicated that capsaicin regulated TJ function through a shared signal pathway, and provided

further evidence showing a vital role of MLC2 in modulation of TJ function. However, the activated MLC2 was not associated with capsaicin-induced TJ expression as evidenced by the use of MLC2 kinase inhibitor ML-7, which suggested that capsaicin-induced TRPV1 activation might mediate the expression and function of the TJ proteins via different signaling pathways, ERK1/2 activation was involved in TRPV1-induced TJ expression, whereas MLC2 activation was mainly responsible for TJ permeability.

The interactions between the TJ proteins and the cytoskeleton F-actin have a crucial role in the regulation of paracellular permeability, because they are directly connected in structure. Thus, any disturbance in F-actin can affect TJ structure and thereby altering TJ permeability.[56] Many studies have pointed out that MLC2 phosphorylation induces F-actin reorganization and then increases paracellular permeability due to the impaired interaction with TJ proteins.[27,28] Our results revealed that capsaicin caused an obvious F-actin accumulation in peripheral cell membrane from cytoplasm, and this effect was suppressed by CPZ and ML-7 preincubation, indicating that the activated TRPV1 and MLC2 were responsible for the capsaicin-mediated F-actin redistribution. In addition, peri-apicolateral F-actin was decreased in transplanted glands and recovered after capsaicin treatment, suggesting that F-actin destruction was involved in the hyposecretion of transplanted SMGs, and capsaicin-induced saliva secretion was associated with F-actin redistribution through activation of TRPV1 and MLC2.

In summary, our data provide new evidence that the impairment in TJ structure, expression, and function are involved in hyposecretion of the transplanted SMGs *in vivo*. Activation of TRPV1 increased saliva secretion in hypofunctional glands, at least in part, by increasing TJ expression and diminishing TJ structural and functional injury. We further demonstrate that TRPV1 activation directly upregulated expression of ZO-1, Cldn-3, and -11 in an ERK1/2-dependent manner, as well as increased paracellular permeability of TJs via MLC2 in SMG cells *in vitro* (a schematic drawing is shown in Figure 9). These findings may improve our understanding of the pathogenesis of hypofunctional SMG and reveal the molecular mechanisms involved in TJ-induced saliva secretion in SMGs. The findings also provide new insights into a future therapeutic target for hyposecretion of SMG.

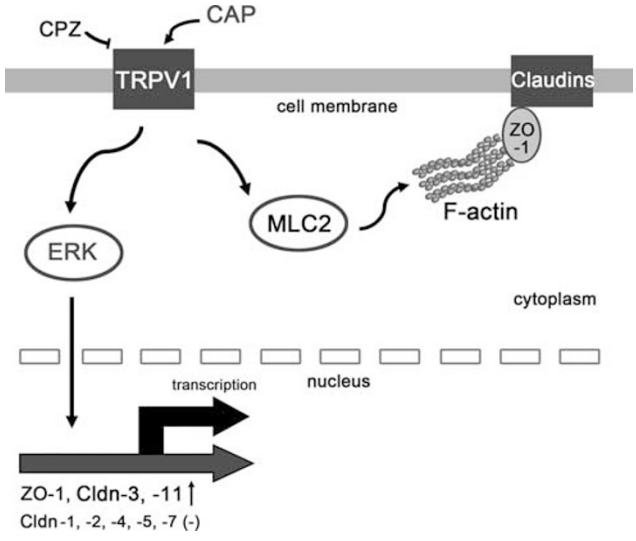

Figure 9 A possible schematic mechanism of transient receptor potential vanilloid subtype 1 (TRPV1) activation on tight junction (TJ) in rabbit submandibular glands (SMGs). Shown are the possible signaling pathways involving extracellular signal-regulated kinase (ERK) and myosin light chain 2 (MLC2) in regulating the TJ expression and function via TRPV1 activation.

Supplementary Information accompanies the paper on the Laboratory Investigation website (http://www.laboratoryinvestigation.org)

ACKNOWLEDGEMENTS

This study was supported by the National Nature Science Foundation of China (Nos. 30730102, 81070847, 30700949); National Supporting Program for Science and Technology (No. 2007BAI18B11). We thank Marguerite Meitzler, professional writer/editor, and Verma Walker, MLIS at NIH Library Editing Service, National Institutes of Health, USA, for reviewing this manuscript.

DISCLOSURE/CONFLICT OF INTEREST

The authors declare no conflict of interest.

1. Tsukita S, Furuse M, Itoh M. Multifunctional strands in tight junctions. Nat Rev Mol Cell Biol 2001;2:285–293.
2. Mitic LL, Anderson JM. Molecular architecture of tight junctions. Annu Rev Physiol 1998;60:121–142.
3. Coyne CB, Vanhook MK, Gambling TM, *et al.* Regulation of airway tight junctions by proinflammatory cytokines. Mol Biol Cell 2002;13:3218–3234.
4. Roxas JL, Koutsouris A, Bellmeyer A, *et al.* Enterohemorrhagic E. coli alters murine intestinal epithelial tight junction protein expression and barrier function in a Shiga toxin independent manner. Lab Invest 2010;90:1152–1168.
5. Peerapen P, Thongboonkerd V. Effects of calcium oxalate monohydrate crystals on expression and function of tight junction of renal tubular epithelial cells. Lab Invest 2011;91:97–105.
6. Schreibelt G, Kooij G, Reijerkerk A, *et al.* Reactive oxygen species alter brain endothelial tight junction dynamics via RhoA, PI3 kinase, and PKB signaling. FASEB J 2007;21:3666–3676.
7. Lourenço SV, Coutinho-Camillo CM, Buim ME, *et al.* Human salivary gland branching morphogenesis: morphological localization of claudins and its parallel relation with developmental stages revealed by expression of cytoskeleton and secretion markers. Histochem Cell Biol 2007;128:361–369.
8. Peppi M, Ghabriel MN. Tissue-specific expression of the tight junction proteins claudins and occludin in the rat salivary tissue. J Anat 2004;205:257–266.
9. Mitsui R, Fujita-Yoshigaki J, Narita T, *et al.* Maintenance of paracellular barrier function by insulin-like growth factor-I in submandibular gland cell. Arch Oral Biol 2010;55:963–939.
10. Hashizume A, Ueno T, Furuse M, *et al.* Expression patterns of claudin family of tight junction membrane proteins in developing mouse submandibular gland. Dev Dyn 2004;231:425–431.
11. Hieda Y, Iwai K, Morita T, *et al.* Mouse embryonic submandibular gland epithelium loses its tissue integrity during early branching morphogenesis. Dev Dyn 1996;207:395–403.
12. Ekström J. Role of nonadrenergic, norcholinergic autonomic transmitters in salivary glandular activities *in vivo*. In: Garrett JR, Ekström J, Anderson LC (eds). Neural Mechanisms of Salivary Glands Secretion (Front Oral Biol). Karger: Basel, 1999, pp 94–130.

13. Caterina MJ, Schumacher MA, Tominaga M, *et al.* The capsaicin receptor: a heat-activated ion channel in the pain pathway. Nature 1997;389:816–824.
14. Ding QW, Zhang Y, Wang Y, *et al.* Functional vanilloid receptor-1 in human submandibular glands. J Dent Res 2010;89:711–716.
15. Zhang Y, Xiang B, Li YM, *et al.* Expression and characteristics of vanilloid receptor 1 in the rabbit submandibular gland. Biochem Biophys Res Commun 2006;345:467–473.
16. Nagumo Y, Han J, Bellila A, *et al.* Cofilin mediates tight-junction opening by redistributing actin and tight-junction proteins. Biochem Biophys Res Commun 2008;377:921–925.
17. Murube-del-Castillo J. Transplantation of salivary gland to the lacrimal basin. Scand J Rheumatol Suppl 1986;61:264–267.
18. Geerling G, Sieg P, Bastian GO, *et al.* Transplantation of the autologous submandibular gland for most severe cases of keratoconjunctivitis sicca. Ophthalmology 1998;105:327–335.
19. Zhang Y, Cong X, Shi L, *et al.* Activation of transient receptor potential vanilloid subtype 1 increases secretion of the hypofunctional, transplanted submandibular gland. Am J Physiol Gastrointest Liver Physiol 2010;299:G54–G62.
20. Segawa A. Tight junction permeability in living cells: dynamic changes directly visualized by confocal laser microscopy. J Electron Microsc 1994;43:290–298.
21. Xiang B, Zhang Y, Li YM, *et al.* Effects of phenylephrine on transplanted submandibular gland. J Dent Res 2006;85:1106–1111.
22. López-Jornet P, Camacho-Alonso F, Bermejo-Fenoll A. A simple test for salivary gland hypofunction using oral Schirmer's test. J Oral Pathol Med 2006;35:244–248.
23. Nighot PK, Blikslager AT. ClC-2 regulates mucosal barrier function associated with structural changes to the villus and epithelial tight junction. Am J Physiol Gastrointest Liver Physiol 2010; 299:G499–G456.
24. Patrick DM, Leone AK, Shellenberger JJ, *et al.* Proinflammatory cytokines tumor necrosis factor-alpha and interferon-gamma modulate epithelial barrier function in Madin-Darby canine kidney cells through mitogen activated protein kinase signaling. BMC Physiol 2006;6:2.
25. Feldman G, Kiely B, Martin N, *et al.* Role for TGF-beta in cyclosporine-induced modulation of renal epithelial barrier function. J Am Soc Nephrol 2007;18:1662–1671.
26. Kinugasa T, Sakaguchi T, Gu X, *et al.* Claudins regulate the intestinal barrier in response to immune mediators. Gastroenterology 2000;118:1001–1011.
27. Hecht G, Pestic L, Nikcevic G, *et al.* Expression of the catalytic domain of myosin light chain kinase increases paracellular permeability. Am J Physiol 1996;271:C1678–C1684.
28. Shen L, Black ED, Witkowski ED, *et al.* Myosin light chain phosphorylation regulates barrier function by remodeling tight junction structure. J Cell Sci 2006;119:2095–2106.
29. Ma T, Song Y, Gillespie A, *et al.* Defective secretion of saliva in transgenic mice lacking aquaporin-5 water channels. J Biol Chem 1999;274:20071–20074.
30. Hashimoto S, Murakami M. Morphological evidence of paracellular transport in perfused rat submandibular glands. J Med Invest 2009;56(Suppl):395–397.
31. Murakami M, Shachar-Hill B, Steward MC, *et al.* The paracellular component of water flow in the rat submandibular salivary gland. J Physiol 2001;537:899–906.
32. Veronesi B, Carter JD, Devlin RB, *et al.* Neuropeptides and capsaicin stimulate the release of inflammatory cytokines in a human bronchial epithelial cell line. Neuropeptides 1999;33:447–456.
33. Birder LA, Kanai AJ, de Groat WC, *et al.* Vanilloid receptor expression suggests a sensory role for urinary bladder epithelial cells. Proc Natl Acad Sci USA 2001;98:13396–13401.
34. Inoue K, Koizumi S, Fuziwara S, *et al.* Functional vanilloid receptors in cultured normal human epidermal keratinocytes. Biochem Biophys Res Commun 2002;291:124–129.
35. Baker OJ, Camden JM, Redman RS, *et al.* Proinflammatory cytokines tumor necrosis factor-alpha and interferon-gamma alter tight junction structure and function in the rat parotid gland Par-C10 cell line. Am J Physiol Cell Physiol 2008;295:C1191–C1201.
36. Kawedia JD, Nieman ML, Boivin GP, *et al.* Interaction between transcellular and paracellular water transport pathways through Aquaporin 5 and the tight junction complex. Proc Natl Acad Sci USA 2007;104:3621–3626.
37. Ewert P, Aguilera S, Alliende C, *et al.* Disruption of tight junction structure in salivary glands from Sjögren's syndrome patients is linked to proinflammatory cytokine exposure. Arthritis Rheum 2010;62:1280–1289.
38. Ko JA, Murata S, Nishida T. Up-regulation of the tight-junction protein ZO-1 by substance P and IGF-1 in A431 cells. Cell Biochem Funct 2009;27:388–394.
39. Georgiadis A, Tschernutter M, Bainbridge JW, *et al.* The tight junction associated signalling proteins ZO-1 and ZONAB regulate retinal pigment epithelium homeostasis in mice. PLoS One 2010;5: e15730.
40. McNeil E, Capaldo CT, Macara IG. Zonula occludens-1 function in the assembly of tight junction in Madin-Darby canine kidney epithelial cells. Mol Biol Cell 2006;17:1922–1932.
41. Furuse M, Furuse K, Sasaki H, *et al.* Conversion of zonulae occludentes from tight to leaky strand type by introducing claudin-2 into Madin-Darby canine kidney I cells. J Cell Biol 2001;153:263–272.
42. Hashimoto K, Oshima T, Tomita T, *et al.* Oxidative stress induces gastric epithelial permeability through claudin-3. Biochem Biophys Res Commun 2008;376:154–157.
43. Gow A, Southwood CM, Li JS, *et al.* CNS myelin and sertoli cell tight junction strands are absent in OSP/claudin-11 null mice. Cell 1999;99:649–659.
44. Morita K, Sasaki H, Fujimoto K, *et al.* Claudin-11/OSP-based tight junctions of myelin sheaths in brain Sertoli cells in testis. J Cell Biol 1999;145:579–588.
45. Gow A, Davies C, Southwood CM, *et al.* Deafness in Claudin 11-null mice reveals the critical contribution of basal cell tight junctions to stria vascularis function. J Neurosci 2004;24:7051–7062.
46. Anderberg EK, Lindmark T, Artursson P. Sodium caprate elicits dilatations in human intestinal tight junctions and enhances drug absorption by the paracellular route. Pharm Res 1993;10: 857–864.
47. Kikuchi K, Kawedia J, Menon AG, *et al.* The structure of tight junctions in mouse submandibular gland. Anat Rec 2010;293: 141–149.
48. Ikari A, Atomi K, Takiquchi A, *et al.* Epidermal growth factor increases claudin-4 expression mediated by Sp1 elevation in MDCK cells. Biochem Biophys Res Commun 2009;384:306–310.
49. Betanzos A, Huerta M, Lopez-Bayghen E, *et al.* The tight junction protein ZO-2 associates with Jun, Fos, and C/EBP transcription factors in epithelial cells. Exp Cell Res 2004;292:51–66.
50. Ikenouchi J, Matsuda M, Furuse M, *et al.* Regulation of tight junctions during the epithelium-mesenchyme transition: direct repression of the gene expression of claudins/occludin by Snail. J Cell Sci 2003;116: 1959–1967.
51. Yamaguchi H, Kojima T, Ito T, *et al.* Transcriptional control of tight junction proteins via a protein kinase C signal pathway in human telomerase reverse trancriptase-transfected human pancreatic duct epithelial cells. Am J Pathol 2010;177:698–712.
52. Zolotarevsky Y, Hecht G, Koutsouris A, *et al.* A membrane-permeant peptide that inhibits MLC kinase restores barrier function in *in vitro* models of intestinal disease. Gastroenterology 2002;123:163–172.
53. Araki Y, Katoh T, Ogawa A, *et al.* Bile acid modulates transepithelial permeability via the generation of reactive oxygen species in the Caco-2 cell line. Free Radic Biol Med 2005;39:769–780.
54. Turner JR, Rill BK, Carlson SL, *et al.* Physiological regulation of epithelial tight junctions is associated with myosin light-chain phosphorylation. Am J Physiol 1997;273:C1378–C1385.
55. Turner JR, Black ED, Ward J, *et al.* Transepithelial resistance can be regulated by the intestinal brush-border Na(+)/H(+) exchanger NHE3. Am J Physiol Cell Physiol 2000;279:C1918–C1924.
56. Bruewer M, Hopkins AM, Hobert ME, *et al.* RhoA, Rac1, and Cdc42 exert distinct effects on epithelial barrier via selective structural and biochemical modulation of junctional proteins and F-actin. Am J Physiol Cell Physiol 2004;287:C327–C335.